Biobased grafted polyesters prepared by in situ ring-opening polymerization

I. Moura [a,*], R. Nogueira [b], V. Bounor-Legare [c,d], A.V. Machado [a]

[a] Institute for Polymers and Composites/I3N, University of Minho, 4800-058 Guimarães, Portugal

[b] IBB - Institute for Biotechnology and Bioengineering, Centre of Biological Engineering, University of Minho, 4705-057 Braga, Portugal

[c] University of Lyon, University of Lyon 1, Lyon F-69003, France

[d] CNRS UMR5223, Ingénierie des Matériaux Polymères: Laboratoire des Matériaux Polymères et Biomatériaux, F-69622 Villeurbanne, France

Keywords:

Ethyl vinyl acetate copolymer
ε-Caprolactone
Lactide
In situ polymerization
Biodegradable

Abstract

EVA-g-PLA and EVA-g-PCL copolymers were synthesized by in situ polymerization of ε-caprolactone and lactide, in the presence of molten ethylene vinyl acetate (EVA) copolymer, using titanium phenoxide ($Ti(OPh)_4$) as initiator. The materials prepared in a internal batch mixer were characterized by ^1H NMR, SEM, FTIR, rheology, DSC, TGA and SEC and the synthesized copolymers identified through selective extraction. The mechanical performance was characterized by tensile tests and the biodegradability by the biochemical oxygen demand method. The results indicated that approximately 11wt. % of EVA-gPCL and 8wt. % of EVA-g-PLA copolymers were synthesized. Moreover, the increase of the Young modulus was higher for the sample containing EVA-g-PCL. This sample also exhibited the higher biodegradability (36%).

Introduction

In recent years, much concern increased on the deterioration of our environment due to solid waste pollution [1]. Nowadays, the challenge is to replace conventional plastics by biodegradable ones to design materials with good performance, which after use can be susceptible to microbial and environmental degradations, using adequate solid waste management disposal practices, without any adverse environmental impact [2]. The easiest way to solve this problem would be to replace commodity synthetic polymers by biodegradable polymers. However, most biodegradable polymers by itself do not have the performance specifications required for a given application [3]. Thus, it is necessary to develop new routes to enhance the properties of biodegradable polymers.

Aliphatic polyesters are one of the most promising biodegradable materials because they are readily susceptible to biological attack [4]. One example is polylactic acid or polylactide (PLA), which has melting temperature around 160 – 180°C, has received much attention as alternative biodegradable polymer [5]. PLA can be obtained from renewable agricultural sources, because lactic acid monomers can be extracted from the fermentation of crop like corn starch and sugar feed stocks [6]. Its production consumes carbon

dioxide, providing significant energy savings and is recyclable and compostable [7-9]. Therefore, PLA presents advantages over other synthetic materials. Other is poly(ε-caprolactone) (PCL), which can be degraded aerobically by a large number of microorganisms in various microbiological environments [10] and it is compatible with a variety of the polymers. However, the high cost of PCL and low melting temperature have prevented its widespread industrial use [11].

Since blending has been used to develop new polymeric materials with specific properties, this method has also been used to prepare new materials with enhanced biodegradability. Blends of biodegradable polymers with various synthetic polymers have been studied for a variety of industrial applications [12]. Natural and synthetic biodegradable polymers (for example, starch, poly(ε-caprolactone) and polylactic acid) have been blended with non-biodegradable synthetic polymers [13,14,10,15]. The results showed that even though biodegradability can increase, due to polymer incompatibility the specified final properties are not achieved. An alternative approach to produce these materials with enhanced properties would be the synthesis of grafted copolymers. Reactive extrusion based on chemical modification by postpolymerization is an attractive way to synthesize these types of copolymers [16,17]. The amount of grafted copolymer formed depends on many factors: (i) choice of the initiator, that is one of the main controlling factors in the grafting reaction through post-living polymerization (ii) processing conditions (temperature and time), (iii) polymers molar mass, (iv) nature of the reaction and (v) monomer miscibility in the molten matrix [18,19].

Ethylene vinyl acetate (EVA) copolymers have a broad range of industrial applications [20], such as packaging, adhesives, wire, cable and health care. Due to the mechanical properties, these copolymers are used perhaps, in a broadest spectrum of applications of any synthetic polymeric material [21]. Since these copolymers have good properties and high resistance to biodegradation, it would be a challenge to develop new materials based on copolymers of EVA and biodegradable polymers.

In previous studies dedicated to the polymerisation of ε caprolactone and the synthesis of EVA-g-PBT grafted copolymers from in situ polymerization of cyclic butylene terephthalate monomer (cBT) in the presence of molten EVA, the advantages of the

specificity of the ring-opening polymerization initiator was taken. First the study of the ring-opening polymerization of the ε-caprolactone initiated by the titanium phenoxide evidenced that, on average, one phenoxide ligand initiates the ring-opening polymerisation [17]. Second, an increase of the polymer molar mass was observed after complete monomer conversion, with a decrease of phenoxyl ester end groups concentration. Actually, this phenomenon is due to transesterification reactions favoured with end groups in case of polymerization with $\mathrm{Ti(OPh)_4}$. Actually, the C-O bond of phenoxyl ester terminal is more prone to nucleophilic substitution than the $\mathrm{C-O}$ bond in repetitive unit due to the influence of phenyl group on electronic delocalisation. This leads to more selective transfer reactions and consequently to more efficiency for grafting reactions. Due to the aromatic character of this titanium derivative, the transfer reaction of the PBT chain onto the EVA backbone was enhanced as described in a recent paper of Bahloul et al. [16]. The copolymer structure and amount was carefully accessed and then precisely characterized by NMR study.

Thus, the present work aims to prepare grafted copolymers of EVA/PLA and EVA/PCL using in situ polymerization of lactide (LA) and ε-caprolactone ($\varepsilon-\mathrm{CL}$) in the presence of molten EVA. This process will take the advantage of a specific exchange reaction between PLA or PCL end-chain groups and the acetate groups of EVA to increase the probability of grafting and consequently the concentration of the formed copolymer. For the ring-opening polymerization, the length of the polymer chains depend directly on the $[M]/[I_0]$ ratio, where $[M]$ and $[I_0]$ are the monomer and the initiator concentration, respectively. Titanium phenoxide ($\mathrm{Ti(OPh)_4}$) was used for its specificity action in the grafting reactions.

The prepared samples were characterized using several analytical techniques, such as, ^{1}H NMR, GPC, FTIR, rheology, SEM, DSC, TGA and mechanical tests. Biochemical oxygen demand (BOD) was carried out to evaluate the biodegradability.

Experimental

Materials

Ethylene vinyl acetate copolymer (EVA 28-03) with 28wt.% of vinyl acetate ($M_n = 18{,}000\ \mathrm{g\ mol^{-1}}$), supplied by ARKEMA, was used as a synthetic polymer. Polylactide ($M_n = 22{,}000\ \mathrm{g\ mol^{-1}}$), poly(ε caprolactone) ($M_n = 10{,}000\ \mathrm{g\ mol^{-1}}$), lactide ($M = 144\ \mathrm{g\ mol^{-1}}$) and ε-caprolactone ($M = 114\ \mathrm{g\ mol^{-1}}$) were supplied from Sigma Aldrich. Titanium phenoxide ($\mathrm{Ti(OPh)_4}$), used initiator, was prepared according to procedure developed by Cayuela et al. [17]. The sample composition is presented in Table 1. For specific comparison, the $[M]/[I_0]$ ratio, where $[M]$ and $[I_0]$ are the monomer and the initiator concentration were chosen to target an in situ PCL and PLA molar mass similar to the commercial polymers used.

Reactive blending

Polymer pellets were dried in a vacuum oven at 25°C for 12 h before use.

Blends of EVA with PLA and EVA with PCL and in situ polymerization of LA with EVA and $\varepsilon-\mathrm{CL}$ with EVA were performed in a Haake batch mixer (Rheocord 90; volume 60 mL),

equipped with two rotors running in a counter-rotating way. The rotor speed was 50 rpm and the set temperature was 160°C. To prepare the blends, the dried components were pre-mixed and introduced together in the mixer. For the in situ polymerization the following procedure was adopted, first the EVA pellets were introduced into the hot mixer, after melting, the monomer and initiator were added simultaneously. Titanium phenoxide was collected in an argon atmosphere, to prevent hydrolysis reaction. In both cases, blends and in situ polymerization, the rotors were stopped after 15 min of mixing and the total sample was removed.

Material characterization

Extractions of copolymer

The EVA-g-PCL and EVA-g-PLA copolymers produced through in situ polymerization were isolated from the homopolymers according to the following method described below and summarized in Fig. 1.

Solubility tests showed that EVA was soluble in hot toluene, but insoluble in acetone. Conversely, PLA and PCL were soluble in acetone at room temperature but insoluble in hot toluene. Thus, two grams of each sample were added to 160 mL acetone and stirred at room temperature for 5 days, approximately. After, the suspension obtained was filtered. The clear solution was precipitated in methanol and the resulting precipitate was dried until constant mass. This product is referred to as fraction 1 (PLA or PCL). The insoluble fraction of the first filtration was extracted in hot toluene during 3 days. The solution obtained was filtered, then evaporated, in a rotational evaporator, and dried. The fraction obtained is referred to as fraction 2 (EVA). The residue of this second extraction was washed with methanol and subsequently dried. This residue composes the third fraction, i.e., the copolymer.

Structural characterization

2.3.2.1. ^{1}H NMR. High resolution liquid ^{1}H NMR spectroscopy was carried out with a Bruker AC 250 instrument at 250 MHz for ^{1}H. Deuterated chloroform, $CDCl_3$ was used as solvent for analysis. Chemical shifts values (δ) are in ppm with reference to internal tetramethylsilane (TMS).
2.3.2.2. Rheological properties. Oscillatory rheological measurements of original polymers and produced samples were carried out in a AR - G2 rotational rheometer at 160°C using a

Table 1
Samples composition.

Sample	EVA (wt.%)	PLA (wt.%)	PCL (wt.%)	-LA (wt.%)	ε-CL (wt.%)	$Ti(OPh)_4$(wt.%)	[M]/[I_0]
1	60	40	0	0	0	0	0
2	60	0	40	0	0	0	0
3	59.5	0	0	39.5	0	1.0	117

4	59.5	0	0	0	39.5	1.0	141

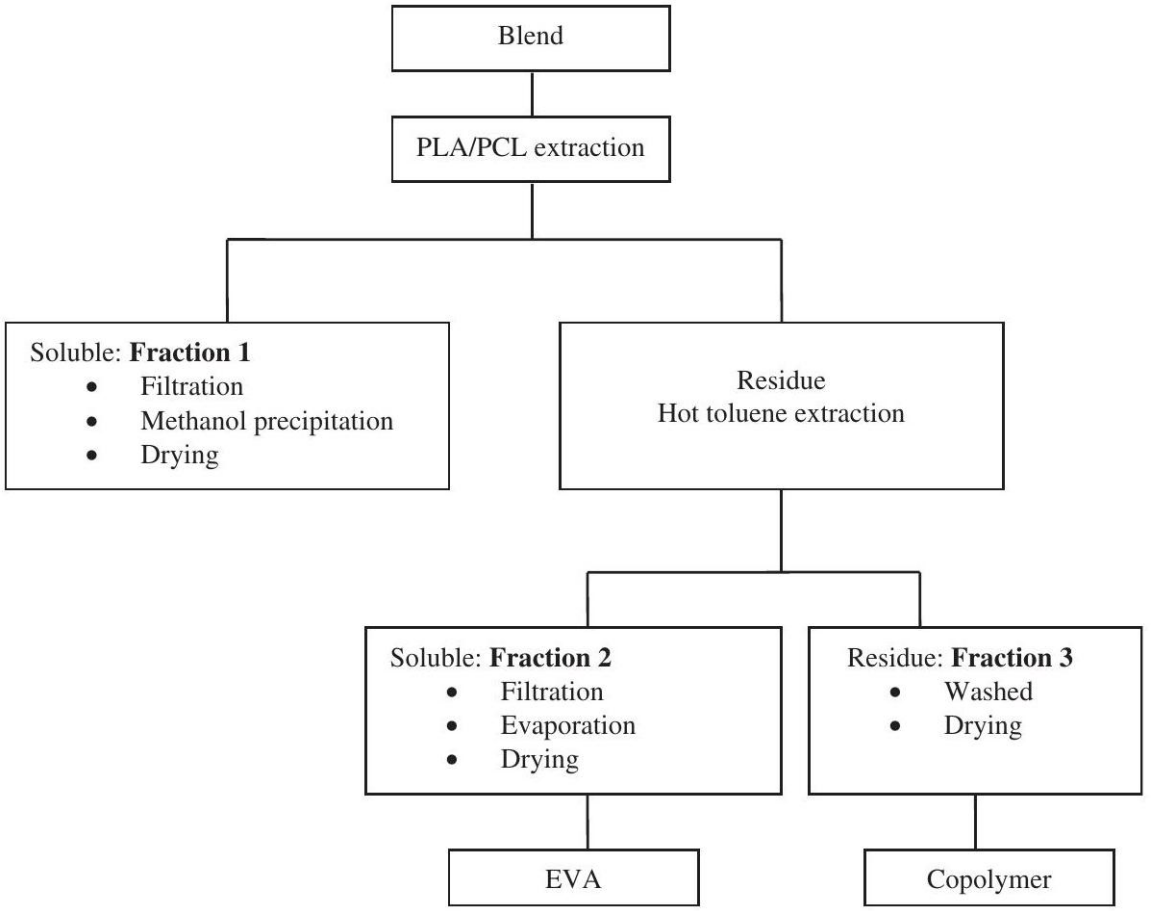

Fig. 1. Extraction scheme of EVA-g-PLA and EVA-g-PCL copolymers. parallel-plate geometry. The gap and diameter of the plates were 1 mm and 4.0 cm , respectively. A frequency sweep from 0.01 to 100 Hz under constant strain was performed for each sample.
2.3.2.3. TGA and DSC. All samples were analyzed using a TA Q500 thermobalance operating under a nitrogen flow atmosphere (50 mL/min). Samples were heated from 30°C to 600°C at a heating rate of 10°C/min.

Thermal properties of all samples were measured using TA Instruments differential scanning calorimeter (DSC 2920). Samples were heated from 25°C to 200°C at a heating rate of 10°C/min, cooled from 200°C to room temperature at the same rate, under liquid nitrogen. The crystallinity degree (X_c) was calculated by the ratio of ΔH_f (the apparent melt enthalpy indicated in DSC curves as melting enthalpy per gram) corresponding toomponent and Δ_f^0 (the melt enthalpy per gram of the component in its theoretically completely crystalline state).
2.3.2.4. SEC. The number average molar mass ($\bar{M}_n$), the mass average molar mass ($\bar{M}_n$) and the polydispersity (I_p) were measured by size exclusion chromatography. Solutions were prepared in chloroform (99.9%) and prefiltered on filter plate (hydrophobic polytetrafluoroethylene, 0.45μ m pore size) before injection. The SEC apparatus was equipped with 2 Waters Ultrastyragel columns (HR1 and HR4; inner diameter = 7.8 mm,

length = 300 mm and particle size = 5μ m) and a Waters R410 refractometer detector. Chloroform was used as eluent with a flow rate of 1 mL/min and at 22°C. The calibration curve was previously obtained with polystyrene standards.

2.3.2.5. SEM. After fracture of the samples in liquid nitrogen and gold plating, the morphology of the samples was studied using a Jeol JSM 6310F Scanning Electron Microscope.

2.3.2.6. Mechanical properties. Mechanical experiments were performed in a MINIMAT apparatus using a test speed of 0.5 mm/ min , at room temperature and relative humidity of 50%. The tests were performed on 2.5 cm × 0.5 cm rectangular samples in a longitudinal direction. At least six specimens of each sample were tested. Prior to mechanical measurements, films with a thickness of 1.5 mm were prepared by compression molding using the samples that were removed from the mixer.

2.3.2.7. Biodegradability assessment. Biodegradation tests were carried out in aqueous environment under aerobic conditions according to the standard ISO 14851: 1999 (Determination of the ultimate aerobic biodegradability of plastic materials in an aqueous medium) [22,23] which specify a method for determining the biochemical oxygen demand (BOD) in a closed respirometer. Polymers were reduced to powder to create a suspension of the polymer in the test system. The Oxitop system used in the determination of BOD contains an individual number of reactors consisting of glass bottles with a carbon dioxide trap (sodium hydroxide) in the headspace. The bottles are supplied with a magnetic stirrer and sealed with a cap containing an electronic pressure indicator. BOD determinations were carried out in 510 mL bottles containing 62.5 mg of the test blend, 2 mL of inoculum and 50 mL of mineral medium. The mineral medium contained 40 mL/L of solution A (28.25 g/LKH_2PO_4, 146.08 g/LK_2HPO_4), 30 mL/L of solution B (3.36 g/L$CaCl_2 \cdot 2H_2O$, 28.64 g/LNH_4Cl), and 30 mL/L of solution C (3.06 g/L$MgSO_4 \cdot 7H_2O$, 0.7 g/L$FeSO_4 \cdot 7H_2O$, 0.4 g/L$ZnSO_4$). The source of inoculum was activated sludge freshly sampled from a municipal sewage treatment plant. The BOD of the inoculum was determined in blank tests performed only with mineral medium and inoculum. These values were subtracted from the BOD values of the blends to obtain exact values of the degradation activity. Test bottles were incubated at 30°C in the dark with stirring for 20 days. All experiments were carried out in triplicate. The amount of O_2 consumed in polymer's biodegradation (after correction with the blank test) was expressed as a percentage of the theoretical oxygen demand (ThOD). The ThOD expressed as mass of O_2 per mass of polymer was determined by calculating the amount of O_2 necessary for aerobic mineralization of the polymer, i.e. complete oxidation of C to CO_2 [23]. The ThOD of the polymer $n(C_cH_hO_o)$, with a relative molar mass M_r (per monomer), was calculated according to:

$$\text{ThOD} = \left(\frac{31.9988}{M_r}\right)(C + 0.25\text{H} - 0.50)$$

The values of theoretical oxygen demand were calculated based on elemental analysis of each sample (see Table 7).

2.3.2.8. FTIR. FTIR spectra of all samples before and after biodegradation were recorded using a Perkin Elmer 1720 spectrometer in the range of $500 - 4000$ cm^{-1}, using 16 scans and a resolution of 4 cm^{-1}. Non-degraded and biodegraded samples were dissolved in chloroform at 5.0%(w/v) and stirring during an hour. Subsequently, an aliquot of this solution was removed and a portion of it (some drops) was deposited in a sodium chloride cell. After solvent evaporation (approximately 3 min) a thin film was obtained and it was analyzed using a solid film support.

2.3.2.9. Elemental analysis. The composition of all samples was determined by elementary

analysis on a LECO CHNS-932. The amount of carbon, hydrogen and oxygen was determined.

Results and discussion

Copolymer identification

In the present work, authors want to take advantage of the specific exchange reaction between the polyester end-chain and the EVA acetate groups, to increase the probability of grafting and consequently the formation of the copolymer in the blend. Therefore, enhancement of the biodegradability character of these copolymers would be expected.

As described previously when polymerization of the cyclic monomer initiated by the titanium phenoxide takes place in the presence of molten EVA, two transfer reactions may be observed leading to the grafting process as shown in Fig. 2 for $\varepsilon - CL$ (the mechanism is the same for LA). A transfer reaction between the acetate group of the EVA and the $Ti - O -$ Polyester bond results in EVA chain functionalized by $Ti(OPh)_3$ and polyester functionalized by an acetate group (Fig. 2a). Another transfer reaction between this new titanate species and either an ester function of polyester chain (Fig. 2b-1), or on the phenoxyl ester end-group (Fig. 2b-2), this latter reaction being favored according to the previous explanations, lead to the formation of grafted species.

After extraction, the fraction amount of each polymer for all the samples is summarized in Table 2. All fractions were analyzed by ^1H NMR to get information on its composition. The spectra obtained for fractions 1 and 2 confirmed that only PLA or PCL and EVA were extracted. It also confirms the efficiency of the extraction methods and the solvents choice. As expected for the physical blends, i.e., mixing both homopolymers without any initiator, the homopolymer percentage is in agreement with the theoretical amount.

Samples 3 and 4 obtained by in situ polymerization of LA and ε CL monomers in the presence of molten EVA exhibit an amount of fraction 3 around 8 and 11wt. % for samples 3 and 4, respectively. The characterization of fraction 3 by ^1H NMR, which corresponds to the insoluble compound in acetone and in hot toluene, gives the following information. On the ^1H NMR spectrum of EVA-CL (Fig. 3), the resonance of both EVA and PCL specific protons are easily detectable. The peaks of CH and CH_3 of EVA are at 4.85 and 2.05 ppm and the peaks of the CH_2 of the $CH_2 - O(CO)CH_2$ repetitive unit of PCL are at 2.30 and 4.05 ppm . Besides these main contributions, others new resonance peaks can also be observed by zooming the regions around 4.0 ppm and 2.0 ppm , respectively. One new peak at 5.15 ppm can be detected, which is associated with a $-CH-$ protons resonance and other one at 1.85 ppm , which is associated to an acetate $-CH_3-$ protons resonance. The appearance of these signals, which are not presented in the spectrum of $Ti(OPh)_4$, are consistent with the proposed mechanism. The new acetate groups corresponds to the one created through a transfer reaction between the acetate group of the EVA and the Ti-OPolyester end bond (Fig. 2a) and the CH corresponds to the grafted PCL on the EVA backbone. These results are in agreement with our previous work dedicated to the synthesis of EVA-PCL grafted copolymer [24] and EVA-PBT grafted copolymer [16].

Since oscillatory rheological measurements are very sensitive to molecular changes, the rheological behavior of all prepared samples was characterized using this technique. From

the viscosity values at low frequency (0.1 Hz) presented in Table 3 it is possible to observe that PLA presents the highest value. This can be explained by the low temperature (160°C) selected for the rheological measurements, which is very close to the PLA melting temperature. The addition of a biodegradable polymer to EVA promotes significant changes of viscosity, but, as expected, the samples with PLA have higher values than the ones with PCL. Comparing the viscosity values of the blends and the samples resulting from the in situ polymerization, one can noticed that the values are higher for samples obtained by in situ polymerization. The difference between the values of samples 1 and 3 and samples 2 and 4 can be associated with copolymer formation, which is in agreement with the extractions. As explained by the NMR results, the copolymers formed in samples 3 and 4 are grafted copolymers, resulting from the reactions between the ester groups of EVA and the ester groups of the in situ polymerized LA or ε-CL. As these copolymers have a branching structure, its presence increases the sample viscosity at low frequencies.

Fig. 4 depicts the thermal behavior (weight loss and correspondent derivative) of EVA, PLA, PCL and prepared samples when heated from 30°C to 600°C at a heating rate of 10°C/min, under nitrogen flow atmosphere. EVA exhibits a first mass lost (18.5%) at around 325°C, which can be attributed to the decomposition of the acetate groups due to the release of acetic acid [25]. At approximately 400°C, a second weight lost (81.5%) can be noticed, corresponding to the degradation of the olefinic part of the copolymer ($C-C$ and $C-H$ bonds).

PLA presents a one-step decomposition profile with a single decomposition temperature. This polymer has lower thermal stability than EVA, because its degradation peak is around 346°C and it decomposes completely (0% char residue) at 380°C. Samples 1 and 3 show two degradation transitions, corresponding to the degradation of the two components of the sample. Sample 1, has an intermediate behavior of EVA and PLA, being the first decomposition temperature (361.68°C) close to the one of PLA and second (380°C) close to the one of EVA. Even though, the thermal behavior of sample 3 is similar to sample 1, a slight shift to higher decomposition temperatures can be noticed from the derivative curves. This might be associated with the amount of grafted polymer present in this sample, its branching structure seems to result in a slight increase of the thermal stability [26].

Compared to EVA, PCL also has lower thermal stability, its first decomposition temperature is around 284°C and it is completely decomposed (0% residue) at 450°C (see Fig. 4b)). Samples 2 and 4 exhibit an intermediate behavior between EVA and PCL. The first decomposition temperature of the blend is similar to the one of PCL and it has a second decomposition temperature similar to the second degradation temperature of EVA. However, as it can be observed from the derivative curves, sample 4 presents a slight increase in decomposition temperatures, which, as in the case of

(a)

PhO

(b)

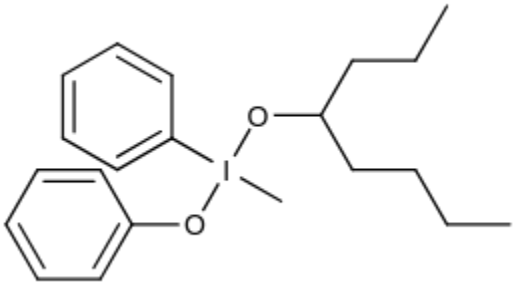

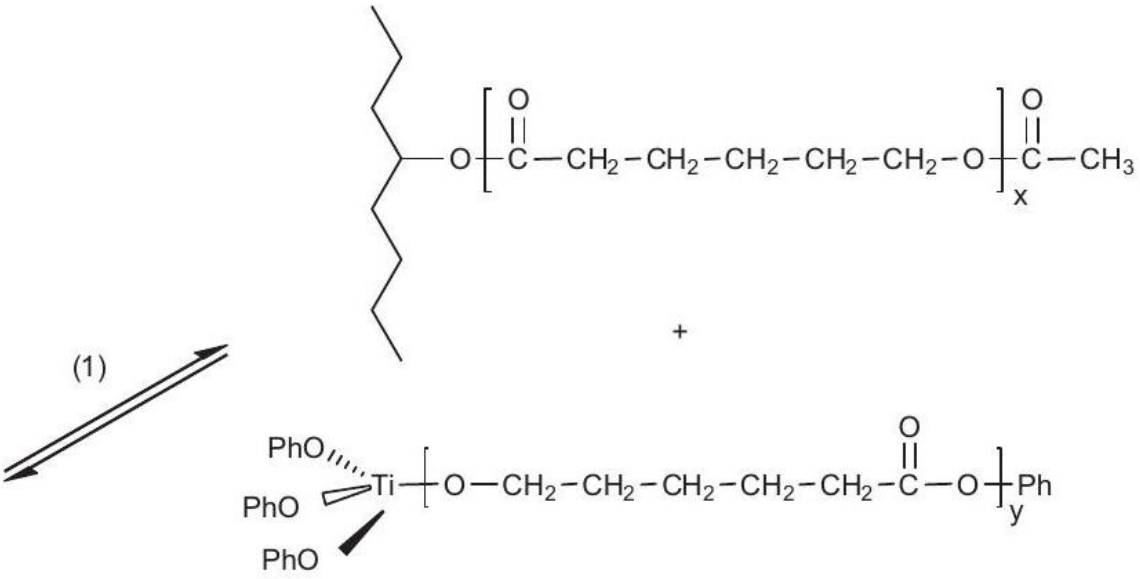
(1)
PhO
PhO
PhO
Ti
Ph

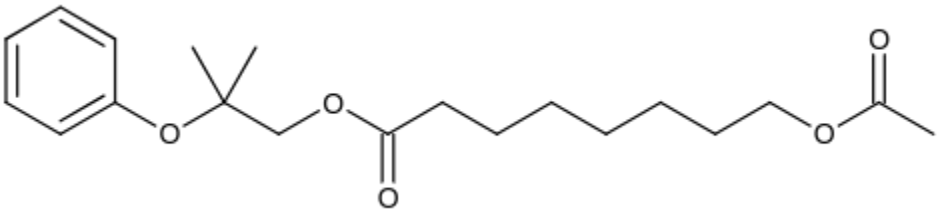

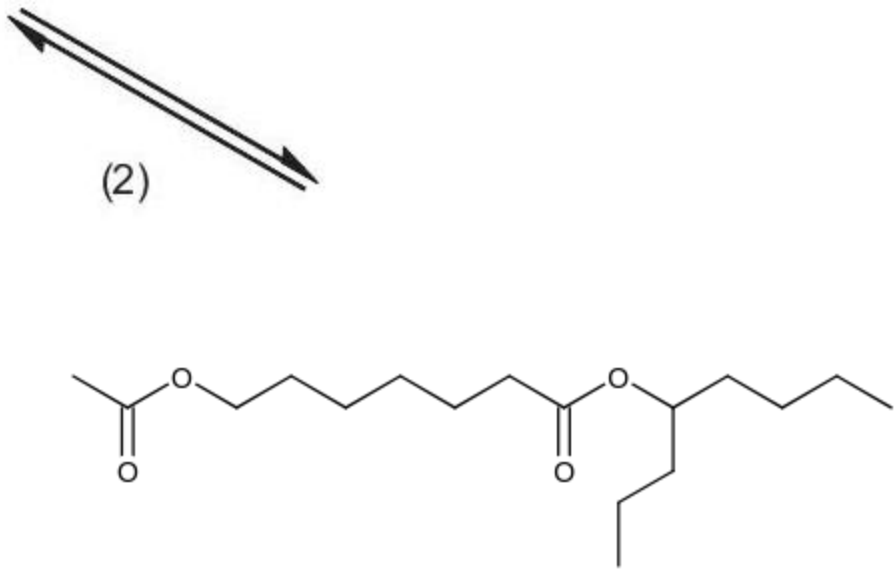

Ti(OPh)4

Fig. 2. Reaction mechanism of EVA-g-PCL copolymer formation (similar mechanism is obtained with the lactide instead of the ε-caprolactone momoner).

Table 2
Fractions amounts extracted.

Sample	Fraction 1 (wt.%)	Fraction 2 (wt.%)	Fraction 3 (wt.%)
1	40	60	0
2	40	60	0
3	36	56	8
4	35	54	11

sample 3, might be associated with the presence of the grafted copolymer.

SEC analysis of all prepared samples and extracted copolymers were performed to confirm copolymer formation. Fig. 5 depicts chromatograms of the neat polymers (EVA, PLA and PCL). Each polymer has a single peak at a certain elution time being the elution time different for all. The results obtained for samples 1 and 2 (Fig. 5a and b) are similar, each analyzed samples presents only one peak. This can be due to the similarity of the molar mass of the neat polymer (18,000,22,000 and 10000 g mol^{-1} for EVA, PLA and PCL, respectively), which after blending are impossible to separate under the conditions used for SEC analyses. Additionally, overlaying samples 1 and 2 with the individual components shows that both samples cover the retention volume of both individual polymers, which indicates that no degradation occurred during blending.

In order to prove that PLA and PCL were grafted onto EVA, SEC data of samples 3 and 4 were overlaid with EVA (Fig. 5c and d). A shift to lower retention volume can be observed for samples 3 and 4 , which is due to an increase of molar mass. These results corroborate the proposed mechanism, the reaction takes place between the ester groups of both copolymers.

Morphology and physical properties

Fig. 6 depicts the morphology of all the samples analyzed by SEM after fracture in liquid nitrogen. The morphology of the polymer blends (Fig. 6a and b) and the samples obtained by in situ polymerization (Fig. 6c and d) consists in a dispersion of particles in the EVA matrix, but significant differences can be noticed among them. Fig. 6a), EVA/PLA blend, which has the lowest magnification, exhibits a coarse morphology, big particles of PLA dispersed in the EVA matrix. The low interfacial adhesion can be perceived from the separation between the blend components. Even though PCL is also dispersed in the EVA matrix, the size of the dispersed phase is much smaller. Since the viscosity of the individual components play an important role on morphology of polymer blends, the differences observed can be associated with differences in melt viscosity. As seen in Table 3, the melt viscosity of PCL is more close to the melt viscosity of EVA than PLA. Another possible explanation can be some compatibility between EVA and PCL.

The dispersed phase of the samples obtained by in situ polymerization is very small when compared to the physical blends morphology, being less pronounced for sample 4. This decrease can be explained by the copolymer formed during reaction, which acts

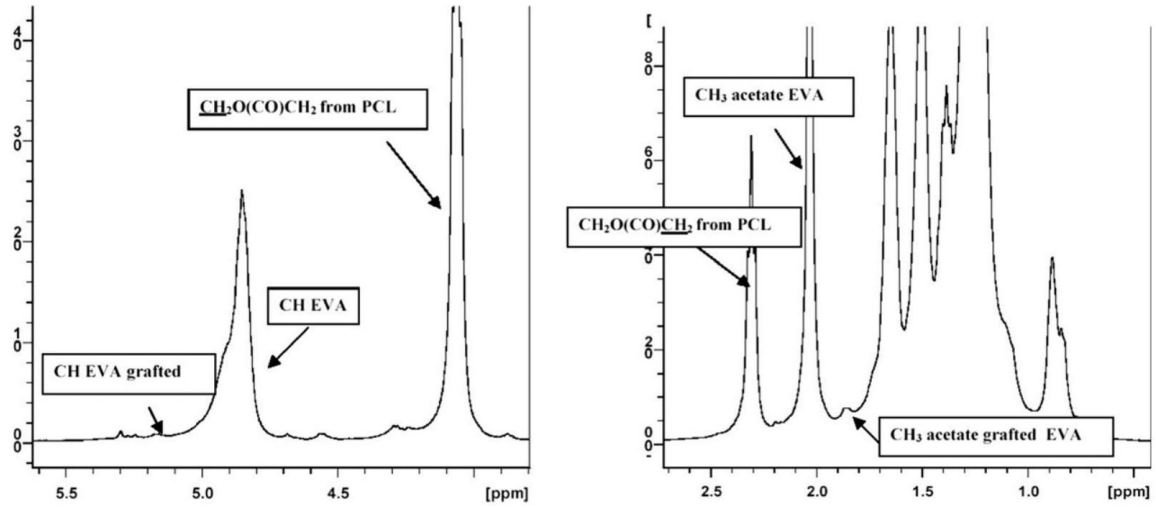

Fig. 3. ^{1}H NMR spectra of EVA-g-PCL.

Table 3
Complex viscosity of initial polymers and prepared samples at a frequency of 0.1 Hz at 160°C.

Sample	η (Pa s)
EVA	105

PLA	1000
PCL	11
1	165
2	52
3	204
4	81

as compatibilizer decreasing the interfacial tension between blends components and consequently the size of the dispersed phase. The morphology of sample 4 can be attributed to the higher copolymer amount.

Tables 4 and 5 present the melting temperature and crystallinity degree, obtained from DSC measurements of neat polymers and prepared samples. The melting temperature and the degree of crystallinity of EVA and PLA of sample 1 is practically the same as the values obtained in the individual measurements. Due to the immiscibility between EVA and PLA, it would be expected that both polymers kept their thermal properties. In sample 2, the melting temperature of EVA changes slightly from 52.1°C to 51.3°C and the melting temperature of PCL changes from 64.4°C to 62.4°C and the crystallinity degree of both polymers decrease. This small difference could be related with some compatibility between EVA and PCL, as it was observed by SEM. The results of samples 3 and 4 present considerable changes in melting temperature and crystallinity degree when compared to individual blend components or samples 1 and 2. This indicates that EVA/PLA and EVA/ PCL samples obtained by in situ polymerization present an enhanced affinity. The decrease of crystallinity degree of samples 3 and 4 is related with the transfer reactions, from which result covalent bonds between PLA or PCL and EVA segments and lead to a lower regularity of the molecular structure. The significant crystallinity decrease observed for PLA in sample 3 is probably due to the PLA structure. This polymer has methyl side groups, which might inhibited the chains connected to EVA to pack and therefore a lower crystallinity degree is achieved. The occurrence of reactions and copolymer formation leads to changes of molecular structures of the polyesters, which promotes changes in melting temperature and crystallinity. Similar results were obtained by Jiang et al. [27] whom synthesized graft copolymer of PCL and EVOH. They attributed the decrease of the melting temperature to the more complex architecture of the copolymer and the relatively low molar mass of PCL side chains.

Tensile strength, modulus and elongation at break of EVA and prepared samples obtained according to the procedure explained in the experimental part are depicted in the Table 6 and Fig. 7. The values for PLA and PCL are not present because under the con-

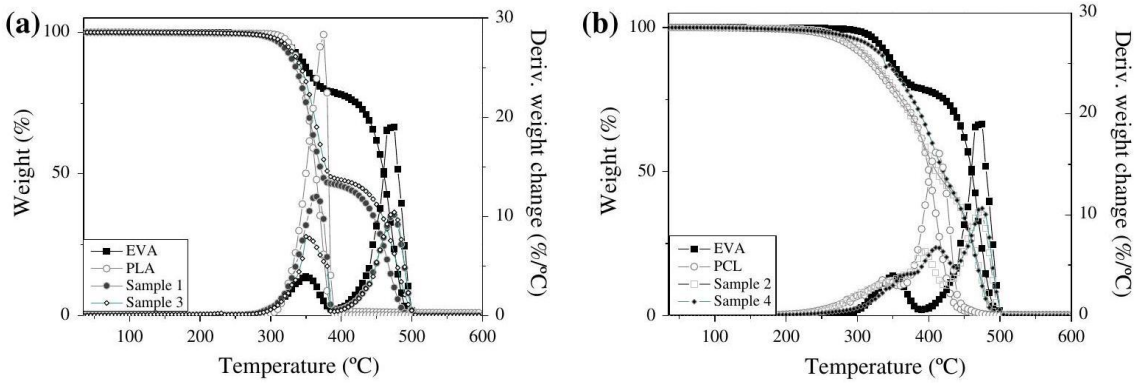

Fig. 4. Thermograms and derivative curves of neat polymers and prepared samples.

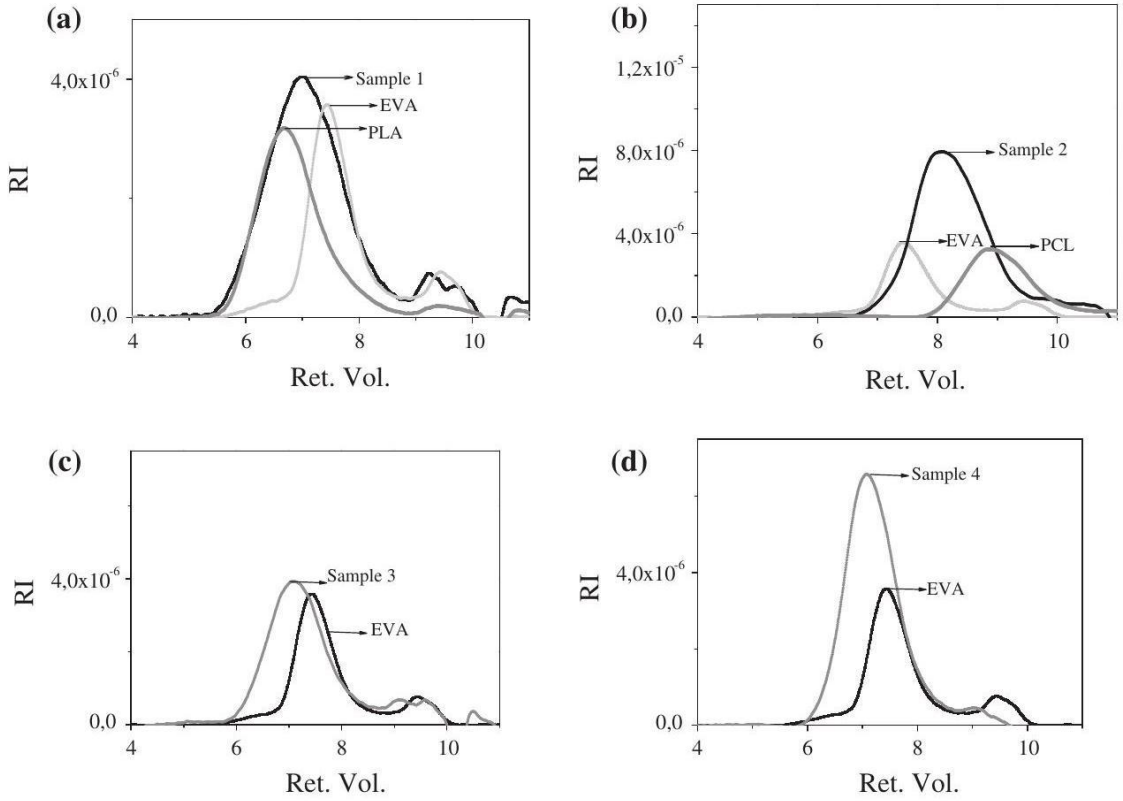

Fig. 5. SEC analysis of neat polymers and prepared samples.

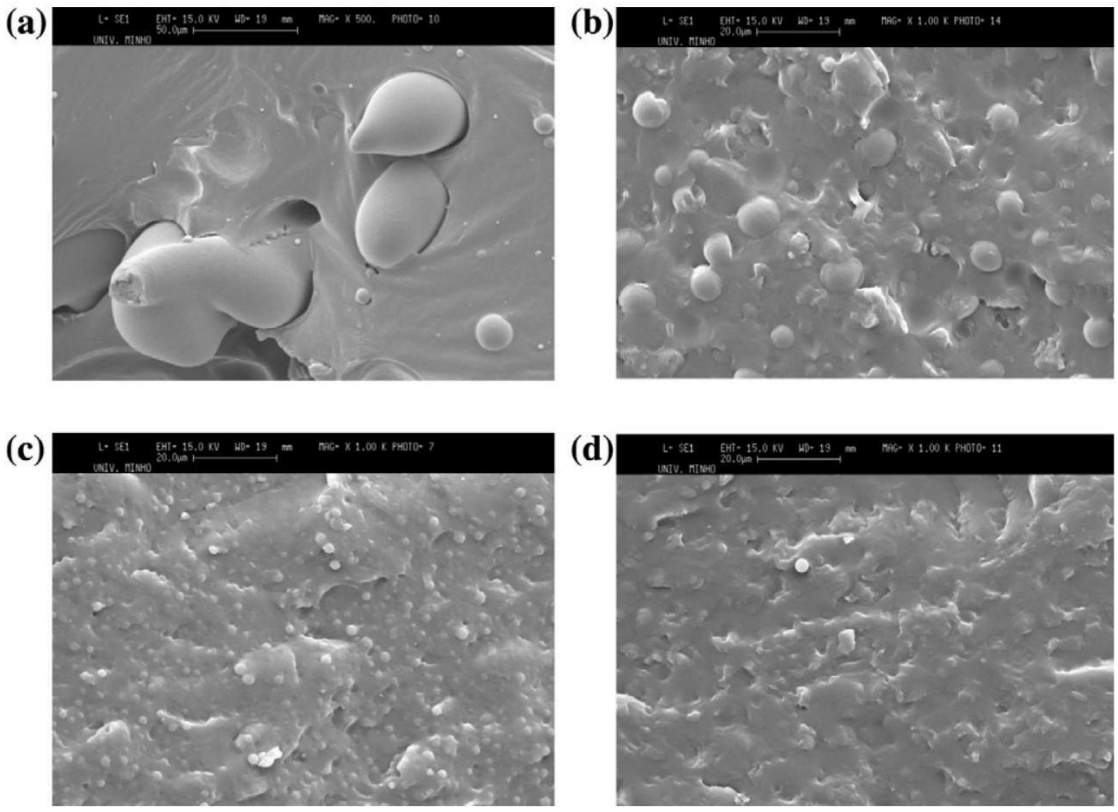

Fig. 6. SEM micrographs of (a) sample 1, (b) sample 2, (c) sample 3 and (d) sample 4.

Table 4

Melting temperature (T_m, ˚C), melting enthalpy (ΔH, J/g) and crystallinity degree (X_c, %) of neat polymers.

Polymer	T_m(˚C)	ΔH(J/g)	ΔH°(J/g)	X_c(%)
EVA	52.1	10.4	44	27.2
PLA	154.6	25.7	93.6	27.5
PCL	64.4	77.1	146	52.8

ditions used to test the samples, these two polymers were very brittle. As it can be observed, the addition of biodegradable polymers to EVA promotes an increase in the tensile strength, i.e., increases of stiffness. Moreover, this enhancement was more pronounced for samples obtained by in situ polymerization than for physical blends. Comparing the physical blends, it can be observed that sample 2 , which is slightly more crystalline than sample 1 , exhibits slightly higher tensile strength (0.27 MPa). This

Table 5
Melting temperatures (T_m, ˚C), melting enthalpy (ΔH, J/g), and crystallinities (X_c, %) of all samples.

Sample	EVA			PLA or PCL		
	T_m(°C)	ΔH(J/g)	X_c(%)	T_m(°C)	ΔH(J/g)	X_c(%)
1	52.1	10.8	24.6	154.7	27.4	26.6
2	51.3	9.4	25.1	62.4	60.8	45.1
3	50.3	11.2	25.6	150.0	17.6	18.8
4	50.7	10.1	23.0	60.4	61.4	42.1

Table 6
Tensile strength and elongation at break of EVA and prepared samples.

Sample	σ(MPa)	ε(%)	Young modulus (MPa)
EVA	0.17 ± 0.02	568 ± 14	1.61 ± 0.49
1	0.10 ± 0.07	361 ± 12	3.98 ± 1.24
2	0.27 ± 0.02	375 ± 24	5.05 ± 2.99
3	0.42 ± 0.03	452 ± 11	11.35 ± 1.63
4	0.47 ± 0.05	611 ± 10	13.23 ± 1.10

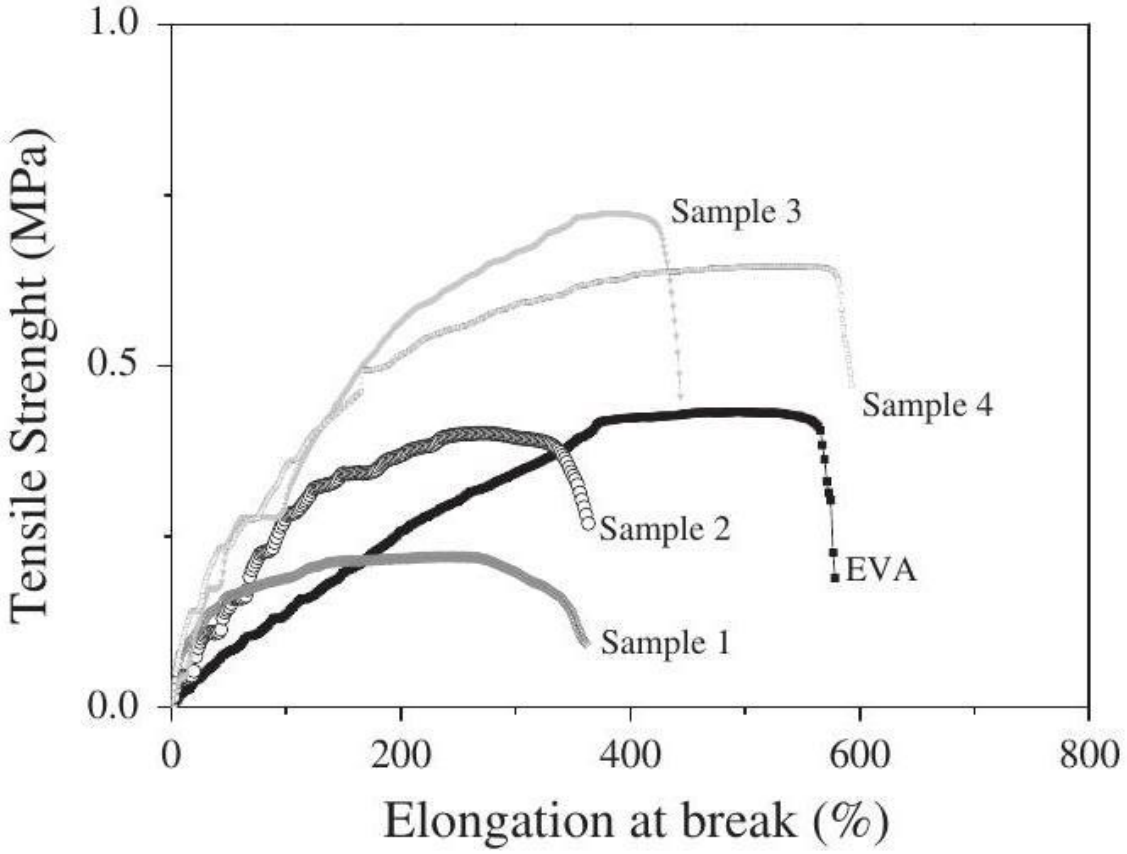

Fig. 7. Tensile properties, at room temperature, of EVA and prepared samples. would be expected since it is well know that crystallinity in polymers is associated with their mechanical properties [28]. This effect can also be seen for samples obtained by in situ polymerization. Sample 4 exhibits a tensile strength of 0.47 MPa while sample 3 has 0.42 MPa and sample 4 is more crystalline than sample 3 (see Table 6).

Conversely, the addition of biodegradable polymers to EVA leads to a decrease of the elongation at break, especially for physical blends. This result can be explained by the formation of two phases with poor compatibility. Nevertheless, this property increases slightly from EVA (568%) to sample 4 (611%). This enhancement can be attributed to the formation of EVA-g-PCL copolymer and its compatibility effect. The effect was less noticeable for sample 3, where EVA-g-PLA where formed, the value in this case was only 452%. The small differences in mechanical properties of the samples prepared by in situ polymerization, can be related with the chemical structure of the copolymer formed and its effect as compatibilizer. SEM micrographs (Fig. 6) clearly show this effect.

Table 7
Elemental analysis of all samples.

Sample	Carbon (%)	Hydrogen (%)	Oxygen (%)	Chemical formula
1	65.3	9.2	25.5	C_4H_6O
2	71.5	11.0	17.5	$C_6H_{10}O$
3	66.0	9.5	24.5	C_4H_6O

4	66.7	10.2	23.2	C_4H_7O

The enhancement of mechanical properties between samples 1 and 3 and 2 and 4 follows morphology improvement.

Biodegradability

The biodegradability of the neat polymers and prepared samples (physical blends and grafted copolymers) was characterized by the biochemical oxygen demand (BOD) method done in a closed respirometer (ISO 14851, 1999). The results obtained during 20 days of biodegradation are depicted in Fig. 8. Among the neat polymers, EVA showed the lowest degree of biodegradability (6.6%), PCL the highest (99.8%), and PLA was in between (37.3%). According to previous studies, reporting that aliphatic polyesters, PCL and PLA, are biodegradable in a wide variety of ecosystems [29], these results were expected. Based on physico-chemical characteristics of both polyesters, it is difficult to explain the fact that PCL was more biodegradable than PLA. On the one hand, the melting temperature of PCL is lower than the one of PLA. As described in literature, polymers with lower melting temperatures are more susceptible to biodegradation because the polymer chains are more flexible and the enzymes can fit more easily into active sites [30]. Also, PCL had a lower molar mass than PLA, which also favored biodegradation [31]. On the other hand, PLA was more amorphous than PCL and based on this parameter PLA was expected to be more biodegradable than PCL, which just did not happen. Thus, prevision of biodegradability based on physico-chemical analyses of the polymers is complex because it depends on several parameters and can lead to wrong results.

It is complex to compare biodegradability results obtained with different methods, using polymers with distinct molar mass. As an example, the biodegradability of PCL under composting conditions (58 °C), 4.3% and 21.6% for PCL with molar mass of 80 kg/mol and 50 kg/mol, respectively, was considerably lower than the one obtained in the present study (99.8%) [32]. A possible explanation for the differences observed derives from the fact that the molar mass of the PCL used in the present study was lower, 10 kg/mol, which enhanced microbial attack. Unfortunately it not possible to compare our PLA data with data from literature because, either the biodegradation were performed at different temperature or the molar mass was unknown. A relatively high biodegradability result for PCL with a molar mass of 43 kg/mol, 80%, was reported in literature obtained with a similar method to the one used in the present study [33]. Blending PLA or PCL with EVA had a positive effect on the biodegradability of the blends obtained, sample 1 (13.3%) and sample 2 (15.1%), compared to EVA (6.6%). Even better biodegradability results were obtained with grafted copolymers, namely sample 3 (18.4%) and sample 4 (36.2%). An increase of biodegradability of grafted copolymers (samples 3 and 4) compared to physical blends (samples 1 and 2) was probably due

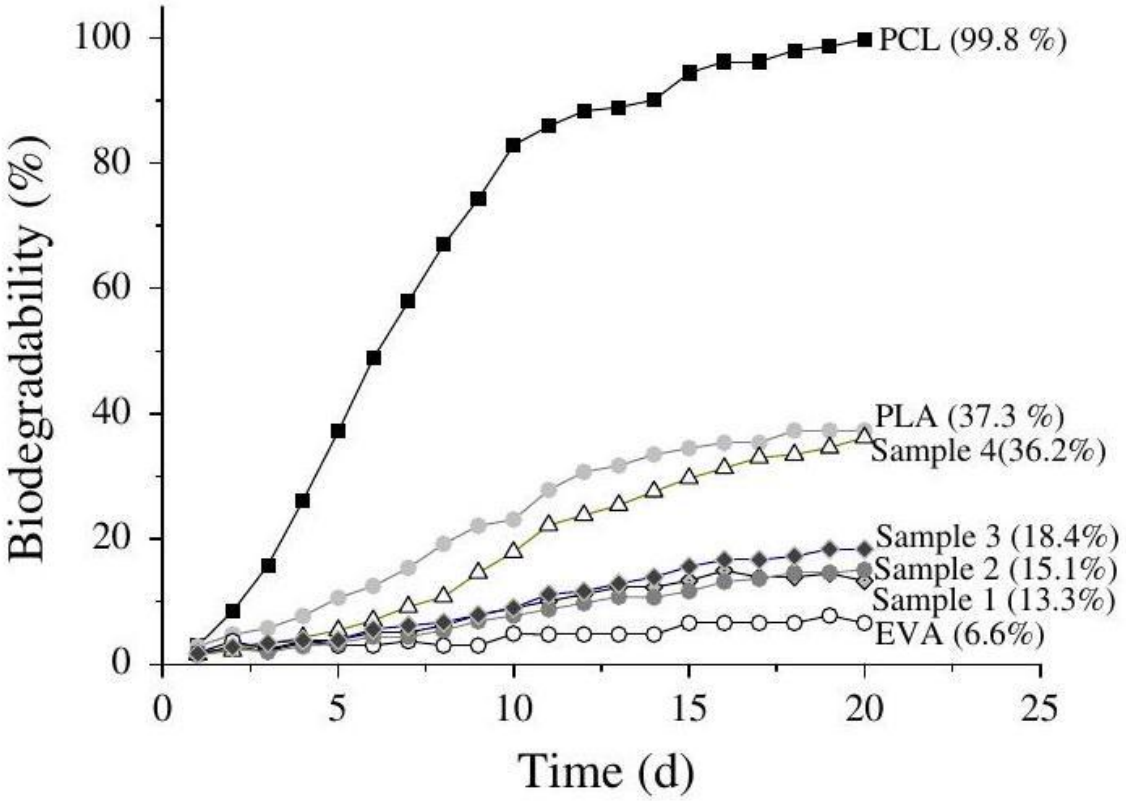

Fig. 8. Biodegradability of polymers and all samples according to ISO 14851(1999).

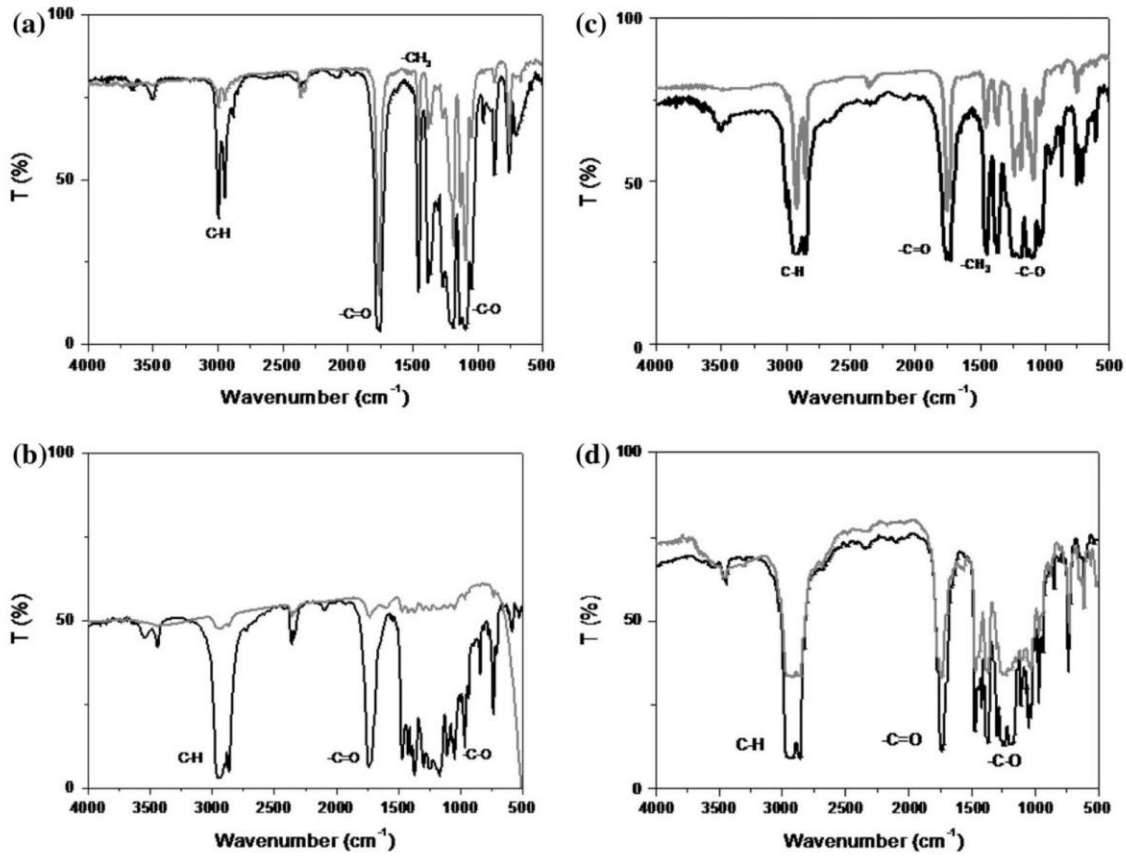

Fig. 9. FTIR spectra of undegraded (black line) and biodegraded (gray line) blends: (a) PLA, (b) PCL, (c) sample 3, and (d) sample 4.
to the simultaneous decrease of crystallinity, melting temperature, and molar mass [34,35].

FTIR analyses of neat polymers were performed to monitor main changes in polymers' backbone after biodegradation. Major changes occurred in the FTIR spectra of PLA (Fig. 9a) and PCL (Fig. 9b) but not in the one of EVA (data not showed). Regarding PLA, transmittance data on a common scale showed that all peaks decreased in size after biodegradation. The reduction in the CHassymetric (2920 cm^{-1}) and CH-symmetric stretches (2850 cm^{-1}) indicated degradation of PLA chains. The decrease of peaks related to carbonyls (1800 cm^{-1} and 1700 cm^{-1}) and ethers (1100 cm^{-1}) indicated chain scission. A reduction of the peak at 1460 cm^{-1} was associated with a decrease of CH_3 side groups. The FTIR spectrum of PCL after biodegradation showed a dramatic change in the polymer backbone evidenced by the reduction of peaks related with CH bonds (3000 – 2800 cm^{-1}), carbonyl (1800 cm^{-1} and 1700 cm^{-1}) and ethers (1100 cm^{-1}) indicating chain scission and, as a consequence, reduction of polymer's molar mass.

FTIR spectra of synthesized PLA polyesters, sample 1 (physical blend, data not showed) and sample 3 (grafted copolymer, Fig. 9c), showed a similar decrease in the intensity of all peaks after biodegradation suggesting a reduction in the molar mass of the polymers. Spectra presented a significant reduction in the intensity of the peaks corresponding to the groups $C-H, C=O$, and $C-O$. This reduction might have been caused by the metabolism of oxygen consuming microorganisms, as suggested by the biodegradability

tests. The FTIR spectrum of sample 2 (physical blend, data not showed) and sample 4 after biodegradation (grafted copolymer, Fig. 9d), showed a reduction in all peaks related to PCL while no major changes were observed in the peaks related to EVA. The decrease in the intensity of the peaks was more pronounced in samples 3 and 4 (containing the grafted copolymers) than in samples 1 and 2 (physical blends), which is in agreement with the biodegradability results. FTIR spectra of biodegraded samples, present a peak at $3500\ cm^{-1}$, which is associated with $O-H$ bonds. A possible explanation for this result is the formation of an alcohol endgroups resulting from polymers biodegradation [36].

Conclusions

Synthesis of EVA-g-PLA and EVA-g-PCL copolymers was investigated by in situ polymerization of ε-caprolactone and lactide in the presence of molten EVA copolymer using as initiator titanium phenoxide. The copolymer structure was characterized by ^{1}H NMR after selective extraction. An amount of approximately 11wt.% for EVA-g-PCL and 8wt.% for EVA-g-PLA was obtained. SEM micrographs showed that the size of the dispersed phase decreased as the amount of copolymer increased, being almost undetectable for the EVA-g-PCL sample. The samples prepared by in situ polymerization, mainly for the EVA-g-PCL sample, exhibit the better mechanical performance.

Biodegradability results, showed that PCL is more biodegradable than PLA, and both more biodegradable than EVA, based on biochemical oxygen demand (ISO 14851:1999). Differences in biodegradability behavior were observed between the physical blends and the samples prepared by in situ polymerization. Moreover, EVA-g-PCL sample was the more biodegradable one. The qualitative results of FTIR spectroscopy of biodegraded polymeric samples confirmed the ones obtained by the standard biodegradability test.

The method used allowed copolymer formation, which even in small amount, promote an enhancement of thermal and mechanical properties of EVA matrix properties and an increase of its degradability. Therefore, in situ polymerization is a promising route to produce biobased materials with good mechanical properties, which could be used in technological applications.

Acknowledgment

The authors would like to thank Portuguese Foundation of Science and Technology (FCT) for financial support (PTDC/AMB/ 73854/2006).

References

[1] S. Lee, J.W. Lee, Korea - Aust. Rheol. J. 17 (2005) 71-77.
[2] A.K. Mohanty, M. Misra, G. Hinrichsen, Macromol. Mater. Eng. 276/277 (2000) 1-24.
[3] Environment Australia, 2002.
[4] S.J. Huang, *Enc. Polym. Sci. Eng. 2 (1985) 220-243.
[5] H. Tsuji, Y.J. Ikada, J. Appl. Polym. Sci. 67 (1998) 405-415.
[6] J. Lunt, Polym. Degrad. Stab. 59 (1998) 145-152.

[7] R.E. Drumright, P.R. Gruber, D.E. Henton, Adv. Mater. 12 (2000) 1841-1846.
[8] R. Auras, B. Harte, S. Selke, Macromol. Biosci. 4 (2004) 835-864.
[9] J.B. Snook, East Lansing (1994) 130.
[10] C. Salom, D. Nava, M.G. Prolongo, R.M. Masegosa, Eur. Polym. J. 42 (2006) 1798-1810.
[11] M.R. Calil, F. Gaboardi, C.G.F. Guedes, D.S. Rosa, Polym. Test. 25 (2006) 597604.
[12] A.V. Machado, I. Moura, F.M. Duarte, G. Botelho, R. Nogueira, A.G. Brito, Int. Polym. Proc. 21 (2007) 512-518.
[13] A. Mohamed, S.H. Gordo, G. Biresaw, Polym. Degrad. Stab. 92 (2007) 11771185.
[14] R. Chandra, R. Rustgi, Prog. Polym. Sci. 23 (1998) 1273-1335.
[15] S.S. Ray, M. Bousmina, Prog. Mater. Sci. 50 (2005) 962-1079.
[16] W. Bahloul, V. Bounor-Legaré, F. Fenouillot, P. Cassagnau, Polymer 50 (2009) 2527-2534.
[17] J. Cayuela, V. Bounor-Legaré, P. Cassagnou, A. Michel, Macromolecules 39 (2006) 1338-1346.
[18] A.V. Machado, J.A. Covas, V. Bounor-Legaré, P. Cassagnau, in: Sabu Thomas, Yang Weimin (Eds.), Advances in Polymer Processing: from Macro- to NanoScales, Woodhead Publishing, 2009.
[19] P. Cassagnau, V. Bounor-Legaré, F. Fenouillot, Int. Polym. Proc. 22 (2007) 218258.
[20] S.P. Tambe, S.K. Singh, M. Patri, D. Kumar, Prog. Org. Coat. 62 (2008) 382-386.
[21] A.M. Henderson, Am. Soc. Test. Mater. 9 (1993) 30-38.
[22] ISO 14851. Determination of the Ultimate Aerobic Biodegradability of Plastic Materials in an Aqueous Medium - Method by Measuring the Oxygen Demand in a Closed Respirometer, 1999, Withdrawn, 2005.
[23] T. Ikejima, A. Cao, N. Yoshie, Y. Inoue, Polym. Degrad. Stab. 62 (1998) 463-469.
[24] M. Valle, Ph.D. Thesis, University of Lyon, Lyon, April 2002.
[25] N.S. Allen, M. Edge, M. Rodriguez, C.M. Liauw, E. Fontan, Polym. Degrad. Stab. 68 (2000) 363-371.
[26] J.-J. Lin, S.-M. Shau, K.-M. Wei, Polym. Degrad. Stab. 70 (2000) 171-184.
[27] H. Jiang, J. He, J. Liu, Y. Yang, Polym. J. 34 (2002) 682-686.
[28] H.C. Ki, O.k. Park, Polymer 42 (2001) 1849-1861.
[29] T. Fujimaki, Polym. Degrad. Stab. 59 (1998) 209-214.
[30] J.-H. Zhao, X.-Q. Wang, J. Zeng, G. Yang, F.-H. Shi, Q. Yan, Polym. Degrad. Stab. 90 (2005) 173-179.
[31] V. Massardier-Nageotte, C. Pestre, T. Cruard-Pradet, R. Bayard, Polym. Degrad. Stab. 91 (2006) 620-627.
[32] D.S. Rosa, R.P. Filho, Q.S.H. Chui, M.R. Calil, C.G.F. Guedes, Eur. Polym. J. 39 (2003) 233-237.
[33] A. Starnecker, M. Menner, Int. Biodeter. Biodegrad. 37 (1996) 85-92.
[34] C. Zhu, K. Xiaodi, Y. You, Z. Zhiqiang, J. Zuo, J. Appl. Polym. Sci. 89 (2003) 848854.
[35] I. Moura, A.V. Machado, R. Nogueira, V. Bounor-Legare, Mater. Sci. Forum. 636/ 637 (2010) 819-824.
[36] I. Moura, A.V. Machado, F.M. Duarte, R. Nogueira, J. Appl. Polym. Sci. 119 (2011) 3338-3346.